

This document is confidential and is proprietary to the American Chemical Society and its authors. Do not copy or disclose without written permission. If you have received this item in error, notify the sender and delete all copies.

Selectivity and Anti-Parkinson's Potential of Thiadiazolidinone RGS4 inhibitors

Journal:	<i>ACS Chemical Neuroscience</i>
Manuscript ID:	cn-2015-000635.R1
Manuscript Type:	Article
Date Submitted by the Author:	n/a
Complete List of Authors:	Blazer, Levi; University of Michigan Medical School, Pharmacology Storaska, Andrew; Michigan State University, Pharmacology and Toxicology Jutkiewicz, Emily; University of Michigan Medical School, Pharmacology Turner, Emma; University of Bristol, School of Chemistry Calcagno, Mariangela; University of Ferrara, Section of Pharmacology Medical Science Wade, Susan; University of Michigan Medical School, Pharmacology Wang, Qin; University of Michigan Medical School, Pharmacology Huang, Xi-Ping; University of North Carolina, Pharmacology Traynor, John; University of Michigan, Department of Pharmacology Husbands, Stephen; University of Bath, Pharmacy and Pharmacology Morari, Michele; University of Ferrara, Medical Science Neubig, Richard; Michigan State University, Pharmacology & Toxicology

SCHOLARONE™
Manuscripts

Selectivity and Anti-Parkinson's Potential of Thiadiazolidinone RGS4 inhibitors

Levi L. Blazer^{1,*}, Andrew J. Storaska^{1,2}, Emily M Jutkiewicz¹, Emma M. Turner³, Mariangela Calcagno⁴, Susan M. Wade¹, Qin Wang¹, Xi-Ping Huang⁵, John R. Traynor¹, Stephen M. Husbands³, Michele Morari⁴, Richard R. Neubig²

¹Department of Pharmacology, University of Michigan Medical School, Ann Arbor, MI 48109,

²Department of Pharmacology and Toxicology, Michigan State University,
East Lansing, MI 48824

³Department of Pharmacy and Pharmacology, University of Bath, Bath, UK.

⁴Section of Pharmacology, Department of Medical Science,
University of Ferrara, Ferrara Italy, 44121.

⁵ National Institute of Mental Health Psychoactive Drug Screening Program (NIMH PDSP),
Department of Pharmacology,
University of North Carolina, Chapel Hill, NC 27599

Correspondence should be addressed to:

Richard R. Neubig, M.D. Ph.D.
Department of Pharmacology & Toxicology
Michigan State University
B440 Life Sciences
1355 Bogue St.
East Lansing, MI 48824

E-mail: rneubig@msu.edu
Phone: 517 353-7145
Fax: 517 353-8915

Keywords: Regulator of G-protein signaling, Parkinson's Disease, PPI, RGS, Protein-Protein interaction, thiadiazolidinone

1
2
3 **Abstract:** Many current therapies target G protein coupled receptors (GPCR), transporters, or
4 ion channels. In addition to directly targeting these proteins, disrupting the protein-protein
5 interactions that localize or regulate their function could enhance selectivity and provide unique
6 pharmacologic actions. Regulators of G protein Signaling (RGS) proteins, especially RGS4,
7 play significant roles in epilepsy and Parkinson's disease. Thiadiazolidinone (TDZD) inhibitors
8 of RGS4 are nanomolar potency blockers of the biochemical actions of RGS4 *in vitro*. Here we
9 demonstrate substantial selectivity (8- to >5000-fold) of CCG-203769 for RGS4 over other
10 RGS proteins. It is also 300-fold selective for RGS4 over GSK-3 β , another target of this class
11 of chemical scaffolds. It does not inhibit the cysteine protease papain at 100 μ M. CCG-203769
12 enhances G α_q -dependent cellular Ca⁺⁺ signaling in an RGS4-dependent manner. TDZD
13 inhibitors also enhance G α_i -dependent δ -OR inhibition of cAMP production in SH-SY-5Y cells
14 which express endogenous receptors and RGS4. Importantly, CCG-203769 potentiates the
15 known RGS4 mechanism of G α_i -dependent muscarinic bradycardia *in vivo*. Furthermore, it
16 reverses raclopride-induced akinesia and bradykinesia in mice, a model of some aspects of
17 the movement disorder in Parkinson's disease. A broad assessment of compound effects
18 revealed minimal off-target effects at concentrations necessary for cellular RGS4 inhibition.
19 These results expand our understanding of the mechanism and specificity of TDZD RGS
20 inhibitors and support the potential for therapeutic targeting of RGS proteins in Parkinson's
21 disease and other neural disorders.
22
23
24
25
26
27
28
29
30
31
32
33
34
35
36
37
38
39
40
41
42
43
44
45
46
47
48
49
50
51
52
53
54
55
56
57
58
59
60

1
2
3
4
5
6 **Introduction:** G protein-coupled receptors (GPCRs) remain key drug targets for therapeutic
7 use⁽¹⁻³⁾. The recent crystal structures of numerous GPCRs have improved the ability to develop
8 subtype-selective ligands^(4, 5). Also, allosteric modulators of GPCRs have provided new
9 degrees of control of signaling with the potential for more refined therapeutic agents^(2, 6). In
10 some cases, however, a single GPCR may mediate both desired and unwanted actions. This
11 is especially true for agonists (e.g. clonidine and adenosine) active in the central nervous
12 system (CNS) where side effects are major limitations to use. It would be highly advantageous
13 to have a mechanism to improve the selectivity of existing GPCR ligands. The downstream
14 actions of GPCRs are modulated by the family of Regulator of G protein Signaling proteins
15 (RGS proteins). Many of the 20 members of this family are abundantly expressed in the brain⁽⁷⁻
16 ¹³⁾. Consequently, they have been proposed as intriguing CNS drug targets⁽⁷⁻¹³⁾. RGS proteins
17 act intracellularly by speeding the deactivation of $G\alpha_i$ and $G\alpha_q$ family G proteins. Inhibition of
18 RGS proteins would thus be expected to potentiate the actions of GPCR agonists.
19 Furthermore, the differential tissue distribution of RGS proteins could provide a novel way to
20 selectively enhance GPCR agonist action in a tissue-specific or neuron-subtype specific
21 manner.
22
23
24
25
26
27
28
29
30
31
32
33
34
35
36
37
38
39
40
41
42

43 RGS4, in particular, assembles in a complex with A1 adenosine receptors and has been
44 proposed to suppress the anticonvulsant action of adenosine⁽¹⁴⁾. Suppression of RGS4 also
45 mediates long-term depression by dopamine through D2 receptors in medium spiny neurons
46 ⁽¹⁵⁾ and RGS4 knockout mice have reduced impairment in 6-OHDA mouse models⁽¹⁵⁾.
47 Furthermore, loss of RGS4 appears to suppress abnormal involuntary movements in mice
48 which represents a model for DOPA-induced dyskinesias⁽¹⁶⁾. According to the recent model⁽¹⁵⁾,
49
50
51
52
53
54
55
56
57
58
59
60

1
2
3 a key action of dopamine is to suppress RGS4 function. Thus, direct, chemical inhibition of the
4
5 hyperactive RGS4 would eliminate the need for dopamine and could provide a novel
6
7 dopamine-independent approach to Parkinson's disease. Consequently, therapeutic targeting
8
9 of RGS4 could be of great interest.
10
11

12
13 It has been challenging to effectively disrupt RGS4/G α and other protein-protein
14
15 interactions, especially in the CNS, but progress is being made⁽¹⁷⁻¹⁹⁾. Indeed, the emerging
16
17 consensus in the field is that effective inhibitors of protein-protein interactions (iPPIs) may not
18
19 meet the "standard" pharmaceutical criteria for drug-like molecules^(20, 21). In spite of this,
20
21 numerous compounds with MW > 500⁽²⁰⁻²²⁾ and several covalent protein modifiers^(23, 24) are
22
23 now in clinical trials. We recently described a series of nanomolar-potency TDZD inhibitors of
24
25 RGS proteins^(25, 26) that can disrupt RGS4 binding to G α subunits in HEK-293 cells. As is seen
26
27 for some other potent iPPIs, they covalently modify cysteine residues in RGS proteins⁽²⁵⁾ but,
28
29 surprisingly, they have high specificity for RGS4 vs. other cysteine-dependent proteins such as
30
31 some kinases and cysteine proteases.
32
33
34
35

36
37 In this study, we assess the specificity of TDZD RGS4 inhibitors and demonstrate
38
39 cellular activity on RGS4 actions on G α_q -mediated cellular Ca⁺⁺ signaling and delta-opioid
40
41 regulation of adenylyl cyclase. Furthermore, CCG-203769 shows *in vivo* activity on muscarinic
42
43 control of heart rate as well as in reversing raclopride-induced Parkinson's-like effects. These
44
45 results represent the first demonstration of *in vivo* effects of TDZD RGS4 inhibitors and
46
47 implicate a potential role in Parkinson's disease and other neuropsychiatric disorders.
48
49
50
51
52
53
54
55
56
57
58
59
60

Results and Discussion:

Identifying selective small molecule inhibitors of protein-protein interactions with activity in the central nervous system remains a key challenge to the expansion of the current therapeutic repertoire beyond receptors, transporters, and kinases. Our previously described RGS4 inhibitor CCG-203769 blocks the RGS4-G α_0 protein-protein interaction *in vitro* with an IC₅₀ value of 17 nM in the Flow Cytometry Protein Interaction Assay (FCPIA, Figure 1A). More importantly, it also displays dramatic selectivity for RGS4 over other RGS proteins (Table 1). The closely related RGS8 is very weakly inhibited (IC₅₀ >60 μ M) providing >4500-fold selectivity for RGS4 (Figure 1A, Table 1). This difference is greater than that seen for our earlier TDZD inhibitor, CCG-50014, which was only ~350-fold selective for RGS4 over RGS8^(25, 26). CCG-203769 inhibits RGS19 with an IC₅₀ of 140 nM (8-fold selective for RGS4) and 6 μ M for RGS16 (350-fold). As with previously reported RGS4 inhibitors, CCG-203769 does not inhibit RGS7, which lacks cysteines in the RGS domain (Table 1).

In addition to inhibiting RGS4/G α binding, CCG-203769 also blocks the GTPase accelerating protein (GAP) activity of RGS4. In single-turnover and steady-state GTPase experiments with G α_0 and G α_{i1} , the rate of GTP hydrolysis is strongly stimulated by RGS4 and this effect is inhibited by CCG-203769 with an IC₅₀ < 1 μ M (Figure. 1B, C). As previously shown for the related TDZD compound CCG-50014⁽²⁵⁾, our new compound is irreversible in non-reducing buffers (Figure 1D). This, as well as the complete lack of effect on RGS7, is consistent with CCG-203769 having the same thiol-modification mechanism as CCG-50014⁽²⁵⁾.

Beyond RGS protein specificity, CCG-203769 is highly selective for RGS4 vs other thiol-dependent proteins. To assess effects on a protein with a catalytic cysteine residue, we

1
2
3 tested CCG-203769 for inhibition of the cysteine protease papain. The general thiol-reactive
4 reagent iodoacetamide strongly inhibited papain-mediated hydrolysis of the fluorescent casein
5 substrate at 30 μM . CCG-203769 at the same concentration had no effect on the protease
6 activity of papain (Figure 1E). Related TDZD compounds are inhibitors of glycogen synthase
7 kinase 3 β ⁽²⁷⁻²⁹⁾. Indeed, they are currently being evaluated in clinical trials for depression and
8 Alzheimer's disease based on this proposed mechanism. Using a radiometric assay, we show
9 that CCG-203769 inhibits GSK-3 β with an IC_{50} value of 5 μM (Figure 1F). This represents 300-
10 fold selectivity of our compound for RGS4 vs. GSK-3 β .
11
12
13
14
15
16
17
18
19
20
21

22 The nanomolar potency on RGS4 *in vitro* translates to respectable cellular activity. We
23 first examined the RGS4/ $\text{G}\alpha_0$ interaction in HEK293 cells. RGS4 is typically present in the
24 cytoplasm but translocates to the membrane when co-expressed with a $\text{G}\alpha$ subunit as
25 demonstrated previously⁽²⁵⁾. Similar to prior results with CCG-50014⁽²⁵⁾, CCG-203769 also
26 reverses the $\text{G}\alpha_0$ -induced membrane translocation of GFP-tagged RGS4 (Figure 2). This
27 demonstrates inhibition of the RGS4- $\text{G}\alpha_0$ interaction in cells. The functional consequences of
28 CCG-203769 were further investigated using a controlled system where induced expression of
29 RGS4 suppresses $\text{G}\alpha_q$ -mediated Ca^{++} signaling activated by the M3 muscarinic receptor.
30 Doxycycline treatment induces RGS4 expression (Figure S1A) reducing the Ca^{++} transient
31 induced by 1 nM carbachol by 63% (Figures S1B&C & 3A). At concentrations of 1 and 3 μM ,
32 CCG-203769 has no effect on intracellular Ca^{++} responses to carbachol stimulation of the M3
33 muscarinic receptor in the absence of RGS4. However, at the same concentrations, it partially
34 reverses the RGS4-mediated muscarinic suppression. At higher concentrations, there may be
35 an off-target effect as the compound appears to inhibit the Ca^{++} transient induced by
36
37
38
39
40
41
42
43
44
45
46
47
48
49
50
51
52
53
54
55
56
57
58
59
60

1
2
3 carbachol. This is similar to previously observed, though more dramatic, effects of CCG-50014
4
5 to disrupt Ca^{++} handling in HEK cells⁽²⁶⁾.
6
7

8 We used SH-SY-5Y neuroblastoma cells to study endogenously expressed RGS and
9
10 opioid receptors. Wang et al⁽³⁰⁾ had previously shown that RGS4 specifically regulates delta-
11
12 opioid receptor (DOP) signaling while having little to no effect on mu-opioid receptor (MOP)
13
14 signaling. CCG-50014 significantly potentiates SNC-80 effects on cAMP accumulation through
15
16 DOP (Figure 3C). Consistent with the previously determined specificity of RGS4, there was no
17
18 significant effect of the compound on MOP-regulated cAMP levels though a trend toward
19
20 potentiation of morphine activity was observed. It is not clear if this is due to effects on RGS4
21
22 or on other RGS proteins in the SH-SY5Y cells to regulate the MOP signal transduction
23
24 cascade. These cellular studies demonstrate that CCG-203769 can potentiate RGS4-regulated
25
26 signaling pathways, regardless of whether they are $\text{G}\alpha_o$ or $\text{G}\alpha_q$ -mediated processes.
27
28
29
30
31

32 Although the TDZD inhibitors have cellular activity, specificity is always a key question
33
34 regarding compounds with a covalent mechanism of action. As noted above, CCG-203769 has
35
36 low potency against GSK-3 β as well as producing no inhibition of the activity of the thiol-
37
38 protease papain at 30 μM . We also assessed off-target effects through broad activity profiling
39
40 at the NIMH PDSP program (University of North Carolina, Chapel Hill)⁽³¹⁾. The compound
41
42 showed no activity at 10 μM against a series of receptors, transporters, etc (Table 2 and S1).
43
44 CCG-203769 had modest activity to inhibit ligand binding in membrane preparations for a
45
46 small subset of the tested systems (α_2 adrenergic, D3 dopamine, and opioid receptors). Using
47
48 the Glowsensor assay^(32, 33) for inhibition of cAMP in cells by these $\text{G}\alpha_{i/o}$ -coupled receptors,
49
50 the TDZD compounds showed no agonist or antagonist activity at concentrations up to 10 μM
51
52 in cells (Table 2).
53
54
55
56
57
58
59
60

1
2
3 A critical step toward translation of new therapeutics is the demonstration of *in vivo*
4 activity as well as avoidance of off-target effects. RGS4 is expressed in the sino-atrial node
5 where it functions to regulate heart rate. Accordingly, RGS4 knockout mice show enhanced
6 carbachol-induced bradycardia⁽³⁴⁾. To determine whether this genetic disruption of RGS4
7 function could be replicated pharmacologically, we tested CCG-203769 for effects on
8 carbachol-mediated bradycardia in conscious, unrestrained rats. Carbachol (0.1 mg/kg, IP)
9 produces a modest decrease in heart rate (Figure 4) compared to a saline vehicle control.
10 CCG-203769 (10 mg/kg, IV) had no significant effect upon heart rate when given alone (Figure
11 4). However, CCG-203769, administered immediately prior to carbachol, significantly
12 potentiated the bradycardic effect (Figure 4, $p < 0.05$, 2-way ANOVA).
13
14
15
16
17
18
19
20
21
22
23
24
25
26

27 Given the functional role of RGS4 in Parkinson's disease models⁽¹⁵⁾, we tested CCG-
28 203769 in a pharmacologic model of D2 antagonist-induced bradykinesia. Raclopride
29 administration in rats causes increased hang time in the bar test (Figure 5A) which was rapidly
30 reversed by doses of CCG-203769 ranging from 0.1-10 mg/kg. The lowest dose, 0.01 mg/kg
31 had no effect while 0.1 mg/kg produced a sub-maximal effect. The higher doses, 1 and 10
32 mg/kg produced equivalent effects. Similarly, the raclopride-induced paw drag in mice (as
33 indicated by reduced numbers of steps), was reversed by 0.1-10 mg/kg CCG-203769 (Figure
34 5B).
35
36
37
38
39
40
41
42
43
44
45

46 In this report, we have characterized the first TDZD RGS inhibitor with physiological
47 activity. CCG-203769, has nanomolar potency against RGS4 and RGS19 *in vitro* and is almost
48 5000-fold selective for RGS4 over the closely related RGS8, making CCG-203769 the most
49 selective RGS4 inhibitor identified to date. As expected, cellular activity is less potent with half-
50 maximal effects occurring in the 1-3 μM range in cells. The inducible RGS4 system provided
51
52
53
54
55
56
57
58
59
60

1
2
3 us with strong evidence of actions on RGS4 rather than other mechanisms that could also
4
5 result in potentiation of the M3 muscarinic signaling response (e.g. M3 muscarinic allosteric
6
7 modulation or effects on cellular Ca⁺⁺ handling). There are, however, additional actions of
8
9 CCG-203769 at higher concentrations that are not fully understood.
10
11

12
13 Despite its cysteine-reactive mechanism of action, CCG-203769 selectively targets
14
15 RGS4 over the known TDZD target GSK3 β , the cysteine protease papain, and a large number
16
17 of receptors and ion channels. The mechanism underlying the RGS selectivity of this
18
19 compound over other cysteine-dependent processes has yet to be fully elucidated, however
20
21 the available data allow for a potential explanation. We previously showed that the covalent
22
23 modification of RGS4 was through opening of the thiadiazolidinone ring to form a disulfide
24
25 bond with cysteine residues on the protein ^(25, 26). This reactivity would presumably provide a
26
27 non-specific mechanism of action. However, dynamic modeling studies ⁽³⁵⁾ indicate that the
28
29 target cysteines on RGS4 are buried in a hydrophobic environment that is only transiently
30
31 accessible to solvent. This suggests that the cysteines in RGS4 may be in a unique
32
33 environment that facilitates the high potency of CCG-203769. Also, in the reducing environment
34
35 of the cell, the disulfide-bonded compound interaction is likely reversible, as shown *in vitro* with
36
37 addition of reducing agents ⁽²⁵⁾. Further studies are required to confirm these hypotheses.
38
39
40
41
42

43
44 In this report, we show that a TDZD RGS4 inhibitor, despite a covalent mechanism of
45
46 action, is very selective for RGS4 over other RGS proteins as well over other sulfhydryl-
47
48 dependent enzymes and a wide range of CNS receptors. Furthermore, it has *in vivo* activity on
49
50 RGS4-dependent control of heart rate and produces beneficial effects in a D2 antagonist-
51
52 mediated akinesia and bradykinesia. In conjunction with the genetic evidence that RGS4
53
54 knockout mice have reduced defects after 6-hydroxy dopamine injury ⁽¹⁵⁾, these results suggest
55
56
57
58
59
60

1
2
3 that CCG-203769 and other related RGS4 inhibitors may have potential as novel
4
5 antiparkinsonian therapies.
6
7
8
9
10
11
12
13
14
15
16
17
18
19
20
21
22
23
24
25
26
27
28
29
30
31
32
33
34
35
36
37
38
39
40
41
42
43
44
45
46
47
48
49
50
51
52
53
54
55
56
57
58
59
60

Materials and Methods:

Sources: Compounds were obtained from sources previously reported for carbachol⁽³⁶⁾; doxycycline, [γ ³²P] GTP⁽²⁵⁾; forskolin, morphine, and SNC80⁽³⁰⁾. Raclopride was purchased from Tocris Bioscience (Bristol, UK). CCG-203769 and CCG-50014 were synthesized as previously described⁽²⁶⁾. Fluo4 NW kits were obtained from (Invitrogen, Carlsbad, CA). RGS proteins and G α subunits were expressed, purified, and labelled as previously described⁽³⁷⁾. GSK-3 β was obtained from Sigma (catalog #G1663). HEK-293T cells expressing the M3 muscarinic receptor and inducible RGS4 (M3-R4 cells) were described previously⁽³⁸⁾.

RGS/G α binding studies: The binding of biotinylated RGS proteins to fluorescently labeled G α_o and the reversibility of RGS4 inhibitor compound actions were measured by Flow Cytometry Protein Interaction Assay (FCPIA) as previously described^(37, 39, 40).

Single-turnover GAP assay: Single turnover GTPase acceleration experiments were performed as previously described using purified his₆-tagged G α_o ⁽²⁵⁾.

Steady-state GAP assay: Steady-state hydrolysis of unlabeled GTP was measured using malachite green in a receptor-independent assay utilizing a mutant G α_{i1} (R178M, A326S)^(38, 41). These mutations facilitate the release of GDP from the enzyme making the GTP hydrolysis step rate-limiting⁽⁴¹⁾. GTP hydrolysis was measured by mixing 6 μ M mutant G α_i with 300 μ M GTP in 100 μ L in 96-well plates in the presence or absence of 200 nM RGS4 and CCG-203769 or DMSO (vehicle control). All assay components were diluted in a buffer comprising 50 mM HEPES at pH 7.4, 100 mM NaCl, 0.01% Lubrol, 5 mM MgCl, and 10 μ g/mL BSA. The reaction was allowed to proceed for 2 hours at room temperature and then was quenched with 60 μ L of an HCl/malachite green dye solution. Immediately after addition of malachite green, 10 μ L of 32% w/v sodium citrate was added as a colorimetric stabilizer, followed by incubation at room temperature for 20 minutes. Released inorganic phosphate was measured as an

1
2
3 increase in absorbance (A_{630}) from the complex of phosphate with malachite green⁽⁴²⁾.

4
5 Background control samples lacking $G\alpha$ were used to determine the rate of non-enzymatic
6
7 GTP hydrolysis which was subtracted.
8
9

10 Papain inhibition: Experiments were performed using fluorescein-isothiocyanate-labeled casein
11
12 as the fluorescent substrate as previously described⁽²⁵⁾.
13
14

15 GSK-3 β inhibition: Purified GSK-3 β (0.5 U, Sigma G1663) was incubated with the indicated
16
17 concentration of compound for 15 minutes at room temperature. Substrate peptide (300 nM,
18
19 Enzo #BML-P151) was added along with 1 mM [γ -³²P] ATP. After a 15 minute incubation at
20
21 30°C, the reaction was quenched by addition of 4 ml of 1% phosphoric acid. The amount of
22
23 phosphorylated peptide was determined by filtration on P81 phosphocellulose filters which
24
25 were washed three times with 4 ml of 1% phosphoric acid to remove unincorporated
26
27 radioactivity. Incorporated radionuclide was quantified by liquid scintillation counting.
28
29
30

31
32 Opioid inhibition of cellular cAMP: SH-SY5Y cells were grown in DMEM containing 10% fetal
33
34 bovine serum and Penicillin (100 units/ml)-Streptomycin (100 μ g/ml) under 5% CO₂ at 37°C.
35
36 Cells were plated into 24-well plates to reach ~ 90% confluency on the day of assay and
37
38 washed once with fresh serum-free medium. Medium was replaced with 1 mM IBMX (3-
39
40 isobutyl-1-methylxanthine) in serum-free medium for 15 minutes at 37°C, and then changed to
41
42 medium containing 1 mM IBMX, 30 μ M forskolin, and 100 nM of either morphine or SNC80
43
44 with or without test compound for 5 min at 37 °C. Reactions were stopped by replacing the
45
46 medium with ice-cold 3% perchloric acid and samples were kept at 4 °C for at least 30
47
48 minutes. An aliquot (0.4 ml) from each sample was removed, neutralized with 0.08 ml of 2.5 M
49
50 KHCO₃, vortexed, and centrifuged at 15,000 x g for 1 minute to pellet the precipitates.
51
52 Accumulated cAMP in a 10-15 μ l aliquot of the supernatant from each sample was measured
53
54
55
56
57
58
59
60

1
2
3 by radioimmunoassay following the manufacturer's instructions (cAMP radioimmunoassay kit,
4 GE Healthcare, Piscataway, NJ). Data are from four separate experiments, each carried out in
5
6 duplicate and calculated as percent inhibition. The basal cAMP accumulation with forskolin
7
8 alone with or without CCG-50014 did not differ.
9
10

11
12 Calcium signaling transients: The M3-R4 cell line with regulated expression of RGS4⁽³⁸⁾ was
13 based upon the HEK-293 Flp-In T-REx cell line (Invitrogen, Carlsbad, CA). It stably expresses
14
15 the muscarinic M3 receptor and has human RGS4 (stabilized C2S mutant, C-terminal HA
16
17 tagged) expression under doxycycline control. Cells were maintained in DMEM supplemented
18
19 with 10% fetal bovine serum and Penicillin (100 units/ml)-Streptomycin (100 µg/ml) under 5%
20
21 CO₂ at 37°C. For experiments, cells were split into 96-well black, clear bottom, poly-D-lysine
22
23 coated microtiter plates (Nunc, Cat. # 152037) at a density of 20,000 cells/well in DMEM
24
25 containing 10% fetal bovine serum and Penicillin (100 units/ml)-Streptomycin (100 µg/ml).
26
27 RGS4 expression was induced by supplementing the medium with 1 µg/mL doxycycline for 24-
28
29 48 hours before experimentation. Cells were loaded with Fluo-4 No-Wash dye (Invitrogen,
30
31 Carlsbad, CA) in loading buffer for 30 minutes at 37°C. Compounds were then added and
32
33 incubated for 30 minutes at room temperature prior to carbachol stimulation. Plates were
34
35 transferred to a FlexStation 3 plate reader (Molecular Devices, Sunnyvale, CA) and carbachol
36
37 (1 nM final) was injected into the wells and the fluorescence intensity was measured as a
38
39 function of time. Peak fluorescence intensity was calculated from a 120 second kinetic
40
41 measurement as a percent increase above the initial fluorescence during the pre-injection
42
43 period.
44
45
46
47
48
49
50
51

52
53 RGS4 membrane localization: Assays were performed as previously described⁽²⁵⁾. Briefly,
54
55 HEK-293T were cells grown to 80-90% confluency in 6-well dishes in DMEM supplemented
56
57
58
59
60

1
2
3 with 10% fetal bovine serum and Penicillin (100 units/ml)-Streptomycin (100 µg/ml) under 5%
4
5 CO₂ at 37°C. RGS and Gα_o were transiently co-transfected (250 ng of a plasmid encoding full-
6
7 length human RGS4 with a C-terminal GFP fusion RGS4pDEST47 and 250 ng of pcDNA3.1 or
8
9 pcDNA3.1 encoding wild-type human Gα_o). Transfected cells were split onto poly-D-lysine
10
11 coated glass coverslips and cultured for 24-48 hours before live cell imaging. Images were
12
13 acquired on an Olympus Fluoview 500 confocal microscope with a 60 x 1.40 numerical aperture
14
15 oil objective. Images were obtained by taking a series of stacks every 0.5 µm through the cell
16
17 and combined into a composite image. The light source for the fluorescence studies was a 488
18
19 nm laser with a 505-525 nm bandpass filter. Images were quantified using NIH ImageJ
20
21 software version 1.43r.
22
23
24
25

26
27 Activity Profiling of CCG-203769: Detailed assay protocols for primary and secondary
28
29 radioligand binding studies as well as functional cell-based assays can be found on the PDSP
30
31 website: <http://pdsp.med.unc.edu/>.
32
33

34 Carbachol-induced bradycardia: These studies were reviewed and approved by the University
35
36 Committee on Use and Care of Animals at the University of Michigan. Under ketamine (90
37
38 mg/kg, i.p.) and xylazine (10 mg/kg, i.p.) anesthesia, rats were implanted with indwelling
39
40 venous catheters (Micro-Renathane tubing, Braintree Scientific Inc., Braintree, MA, USA) and
41
42 telemetric BP and ECG transmitters (Model C50-PXT, Data Sciences, Transoma Medical, Inc.,
43
44 St. Paul, MN, USA) at the same time under aseptic conditions. Venous catheters were inserted
45
46 3 cm into the right or left jugular vein and sutured to the vein and to the surrounding tissue at
47
48 3-4 points to secure catheter placement. The remaining tubing (approximately 9-12 cm) was
49
50 threaded subcutaneously to a dorsal incision and held in place by suture to musculature
51
52 directly below the incision. Telemeters were implanted subcutaneously in the rat and secured
53
54
55
56
57
58
59
60

1
2
3 to the abdominal wall. The catheter extending from the base of the transmitter was placed 3
4
5 cm into the left femoral artery. Electrodes from the bottom of the transmitter were threaded
6
7
8 subcutaneously and one was sutured to the muscle above the xiphoid process and the other
9
10 was sutured to the right of the clavicle. All rats were singly housed and allowed at least 7 days
11
12 to recover before testing.
13
14

15 The telemetry system consisted of battery-operated transmitters and receivers (Data
16
17 Sciences, TransomaMedical, St. Paul, MN, USA). Mean arterial pressure (MAP) and heart rate
18
19 (beats per min, bpm) were acquired using Dataquest A.R.T. 3.01, collected every 10 sec and
20
21 then averaged over 1 minute periods. A rat's home cage was placed in the receiver at least
22
23 one hour prior to testing to allow for habituation. CCG-203769 is an oil and was solublized in
24
25 sterile saline by vigorous vortexing. All compounds were administered *in vivo* in a volume of 1
26
27 ml/kg by routes of administration indicated above. After habituation, rats received CCG-203769
28
29 or saline (by i.v. infusion through the indwelling venous catheter over 30 sec) while freely
30
31 moving in their homecage. One minute later, saline or 0.1 mg/kg carbachol (i.p.) was
32
33 administered. Before and after i.v. infusions, catheters were flushed with approximately 0.5 ml
34
35 of heparinized saline (50 U/ml) to check catheter patency and flush treatments from dead
36
37 space in catheter. Following all experiments, rats were euthanized by i.v. pentobarbital (150
38
39 mg/kg) to ensure catheter patency. Statistical significance was evaluated by 2-way ANOVA
40
41 with a significance cut-off of 0.05.
42
43
44
45
46
47

48 Raclopride-induced movement suppression: These experimental protocols were approved by
49
50 the Italian Ministry of Health (license n. 171/2010-B) and Ethical Committee of the University of
51
52 Ferrara Young male (20-25 g; 8-9 weeks) C57BL/6J mice, were purchased from Harlan Italy
53
54 (S. Pietro al Natisone, Italy) and were housed with free access to food and water with a 12-h
55
56
57
58
59
60

1
2
3 light/dark cycle with lights on between 07:00 and 19:00. Prior to pharmacological testing, mice
4
5 were handled for 1 week by the same operator to reduce stress, and trained daily for a week
6
7 on the behavioral tests until their motor performance became reproducible. On the day of
8
9 experiment drugs were administered systemically (i.p.); CCG-203769 was administered 30 min
10
11 after raclopride.
12
13

14
15 Motor activity was evaluated by means of different behavioral tests (bar and drag)
16
17 specific for different motor abilities, as previously described^(43, 44). The different tests are useful
18
19 to evaluate motor functions under static or dynamic conditions. Akinesia appears as an
20
21 abnormal absence or poverty of movements, that is associated with loss of the ability to move
22
23 the forepaw when placed on blocks (bar test). Bradykinesia is slowness of movement with
24
25 difficulties of adjusting in response to backwards dragging (drag test). The tests were repeated
26
27 in a fixed sequence (bar and drag test) before (control session) and after (30 minutes)
28
29 raclopride injection, then 20 and 90 minutes after CCG-203769 injection.
30
31
32

33
34 The bar test or catalepsy test⁽⁴⁵⁾, measures the ability of the animal to respond to an
35
36 externally imposed static posture. Each mouse was placed gently on a table and the right and
37
38 left forepaws were placed alternately on blocks of increasing heights (1.5, 3 and 6 cm). The
39
40 immobility time (in seconds) on the blocks was recorded (cut-off time 20 seconds per step, 60
41
42 seconds maximum). Time was recorded as total time spent on the blocks. The drag test is a
43
44 modification of the “wheelbarrow” test⁽⁴⁶⁾. Each mouse was gently lifted by the tail (allowing the
45
46 forepaws on the table) and dragged backwards at a constant speed (about 20 cm/sec) for a
47
48 fixed distance (100 cm). The number of touches made by each forepaw was counted by two
49
50 separate observers (mean between the two forepaws).
51
52
53
54
55
56
57
58
59
60

1
2
3 Data are expressed as means \pm SEM of n determinations per group. Statistical analysis
4
5 was performed using one-way repeated measures (RM) ANOVA followed by the Newman-
6
7 Keuls test. P values <0.05 were considered to be statistically significant. Both raclopride and
8
9 CCG-203769 were freshly dissolved in the vehicle just prior to use.
10
11
12
13
14
15
16
17
18
19
20
21
22
23
24
25
26
27
28
29
30
31
32
33
34
35
36
37
38
39
40
41
42
43
44
45
46
47
48
49
50
51
52
53
54
55
56
57
58
59
60

Author Information

Levi Blazer, Andrew Storaska, and Sue Wade designed and performed the biochemical and cell-based assays. Qin Wang and John Traynor designed the opioid functional studies which were performed by Qin Wang. Emily Jutkiewicz and Levi Blazer designed and performed the studies on compound effects on muscarinic bradycardia. Emma Turner and Stephen Husbands designed and synthesized CCG-203769. Mariangela Calcagno and Michele Morari designed and Mariangela Calcagno performed the Parkinson's model studies. Xi-Ping Huang designed and performed the target screening studies at the PDSP. Richard Neubig contributed to the design of the overall project and all individual experiments. He and Levi Blazer wrote the manuscript with text and suggestions contributed by all authors.

Conflicts of Interest

Richard Neubig is founder and owner of Argessin LLC which has licensed rights to TDZD RGS4 inhibitors from the University of Michigan.

Acknowledgements

The authors would like to thank Jian Mei for assistance with the FCPIA studies and Roger Sunahara and John Tesmer for valuable discussions. Funding was provided by NIH RO1 DA023252 (RRN), the Chemical Biology Interface training program NIH T32GM008597 (LLB) and core facilities supported by the Michigan Diabetes Research and Training Center NIH P60 DK020572 and University of Michigan Comprehensive Cancer Center Support Grant NIH P30 CA046592. Receptor binding profiles, and agonist and antagonist functional data was generously provided by the National Institute of Mental Health's Psychoactive Drug Screening Program, Contract # HHSN-271-2013-00017-C (NIMH PDSP). The NIMH PDSP is directed by Bryan L. Roth MD, PhD at the University of North Carolina at Chapel Hill and Project Officer Jamie Driscoll at NIMH, Bethesda MD, USA. For experimental details please refer to the PDSP web site <http://pdsp.med.unc.edu/>.

Supporting Information Available

A brief characterization of the M3-R4 Flp-in cell line is presented as supporting information for the manuscript. This information is available free of charge via the internet at <http://pubs.acs.org/>.

1
2
3 Figure Legends
4

5
6 Figure 1. Biochemical characterization of RGS inhibitors. A) CCG-203769 inhibits RGS4 and
7 RGS8 binding to $G\alpha_o$ in FCPIA in a concentration-dependent manner. *Inset*: chemical structure
8 of CCG-203769. See Table 1 for IC_{50} values. CCG-203769 inhibits the RGS-mediated
9 acceleration of GTPase activity by both B) $G\alpha_o$ in single-turnover and C) $G\alpha_{i1}$ in steady-state
10 GTPase assays. D) CCG-203769 irreversibly inhibits RGS4 binding to $G\alpha_o$ in non-reducing
11 buffers. RGS4-coated beads were treated with 0.5 μ M CCG-203769, extensively washed, and
12 then probed for $G\alpha_o$ binding. E) CCG-203769 (30 μ M) does not inhibit the cysteine protease
13 papain. The positive control compound, iodoacetamide (30 μ M) did effectively inhibit papain
14 activity (see Methods for details). F) CCG-203769 inhibits GSK-3 β with an IC_{50} value of 5 μ M.
15
16 Data are presented as the mean \pm SEM from at least three independent experiments. * $p<0.05$,
17
18
19
20
21
22
23
24
25
26
27
28
29
30
31
32
33
34
35
36
37
38
39
40
41
42
43
44
45
46
47
48
49
50
51
52
53
54
55
56
57
58
59
60
**** $p<0.0001$

35 Figure 2: CCG-203769 inhibits the $G\alpha_o$ -dependent membrane translocation of RGS4 in
36 HEK293T cells. RGS4-GFP generally has a diffuse cytosolic protein expression pattern,
37 however, co-expression with $G\alpha_o$ induces a translocation of the RGS to the cell membrane⁽²⁵⁾.
38
39 A/C) Treatment with DMSO does not modulate the RGS4 membrane localization, while B/D)
40 treatment with CCG-203769 (100 μ M) reverses the membrane translocation of the RGS4.
41
42 Representative data shown from at least three independent experiments with 3-5 cells imaged
43 per experiment. Line scans (C & D) were quantified from a single line perpendicular to the long
44 axis of the cell in pre (Media) & post (DMSO or CCG-203769) treatment images. Pixel intensity
45 was obtained using the NIH ImageJ software version 1.43r.

1
2
3 Figure 3. TDZD RGS4 inhibitors block RGS function in living cells. A) RGS4 induction by
4 doxycycline suppresses the $G\alpha_q$ -mediated calcium transient invoked by activation of the M3
5 muscarinic receptor. CCG-203769 (3 μ M) reverses the effect of RGS4. B) Quantification of the
6 data shown in A, showing that CCG-203769 significantly inhibits the RGS4 modulation M3
7 signaling at 1 and 3 μ M. Data are presented as the mean \pm SEM of three independent
8 experiments. C) δ -opioid receptor signaling in SH-SY5Y neuroblastoma cells is potentiated by
9 the TDZD RGS4 inhibitor. The endogenous δ and μ receptors in SH-SY5Y cells are regulated
10 by endogenous RGS proteins. CCG-50014 (100 μ M) significantly potentiates the cAMP
11 inhibition produced by the δ opioid receptor agonist SNC-80, while only modestly potentiating
12 actions of the μ -opioid receptor agonist morphine. Data are presented as the mean \pm SEM of
13 three independent experiments.* $p < 0.05$; ** $p < 0.01$
14
15
16
17
18
19
20
21
22
23
24
25
26
27
28
29
30
31

32 Figure 4. CCG-203769 potentiates the cardiovascular effects of carbachol in conscious rats.
33 Blood pressure and heart rate of adult Sprague-Dawley rats were monitored via indwelling
34 cardiac transponders. Rats were given CCG-203769 (10mg/kg, i.v.) or saline immediately
35 before administration of saline or carbachol (0.1mg/kg, i.p.). CCG-203769 has no effect on
36 heart rate when administered alone, however it significantly potentiates ($p < 0.05$, 2-way
37 ANOVA) the effect of carbachol (0.1mg/kg). N=6 per condition.
38
39
40
41
42
43
44
45
46
47

48 Figure 5. AntiParkinson's effects of RGS4 inhibitors. Mice were treated with raclopride (1
49 mg/kg i.p.) after baseline assessment in the bar and drag tests (as described in Materials and
50 Methods). A) Akinesia and B) bradykinesia were assessed 30 minutes after raclopride then
51 mice received either DMSO or CCG-203769 at the indicated doses (i.p.). Behavior was
52
53
54
55
56
57
58
59
60

1
2
3 assessed 20 or 90 minutes after DMSO or CCG-203769. Values are mean +/- SEM with
4
5 differences from baseline indicated by ** ($p < 0.01$) and differences from Raclopride + DMSO
6
7 indicated by ## ($p < 0.01$).
8
9
10
11
12
13
14
15
16
17
18
19
20
21
22
23
24
25
26
27
28
29
30
31
32
33
34
35
36
37
38
39
40
41
42
43
44
45
46
47
48
49
50
51
52
53
54
55
56
57
58
59
60

Tables

Table 1. Selectivity of CCG-203769. The binding of RGS proteins to $G\alpha_o$ was measured using FCPIA. CCG-203769 inhibited RGS/ $G\alpha_o$ binding in an RGS-selective manner. Functional data for non-RGS activities are described in the text. Data are presented as mean from three independent experiments performed in duplicate. Fold-selectivity is presented as the ratio of the IC_{50} of CCG-203769 towards a given target versus its IC_{50} against RGS4.

RGS Protein	IC_{50} (μ M)	Fold Selectivity (RGS4)
RGS4	0.017	1
RGS19	0.14	8.2
RGS16	6	350
RGS8	79	4650
RGS7	>100	>6000

GSK3 β	5.4	320
Papain	>100	>6000

Table 2 Specificity analysis of CCG-203769.

The compound was tested for activity in a wide variety of ligand binding or functional assays through the NIH PDSP laboratory. Targets for which activity was found in primary or secondary binding assays were then examined in cell-based functional studies. In the latter, assessment of both agonist and antagonist activity was done. Assay protocols are available on the PDSP web site (<https://pdspdb.unc.edu>).

Target	Biochemical assays		Cellular assays
	Primary Binding (% Inhibition @ 10 μ M)	Secondary Binding (IC ₅₀ nM)	Agonist/Antagonist Potency (EC ₅₀ /IC ₅₀ nM)
5-HT1A,B,D,E; 5-HT2A,B,C, 3, 5A, 7 β -AR1,2,3; α 1-AR A, B, D D2, D4, H1-4; M1-5; Benzodiazepine; GABA-A; DAT, NET, SERT Sigma1,2	<50%	ND	ND
5-HT6	69	>10,000	ND
α 2A adrenergic	97	290	>10,000
α 2B adrenergic	93	2,290	>10,000
α 2C adrenergic	97	140	>10,000
D1 dopamine	54	>10,000	ND
D3 dopamine	84	1,530	>10,000
D5 dopamine	67	>10,000	ND
DOR	53	2,630	>10,000
KOR	90	1,520	>10,000
MOR	54	2,680	>10,000

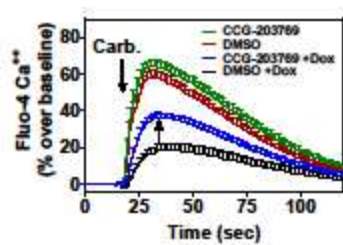
ND = Not determined.

Literature references

1. Carrieri, A., Perez-Nueno, V. I., Lentini, G., and Ritchie, D. W. (2013) Recent trends and future prospects in computational GPCR drug discovery: from virtual screening to polypharmacology, *Curr Top Med Chem* 13, 1069-1097.
2. Nickols, H. H., and Conn, P. J. (2014) Development of allosteric modulators of GPCRs for treatment of CNS disorders, *Neurobiol Dis* 61, 55-71.
3. Shonberg, J., Lopez, L., Scammells, P. J., Christopoulos, A., Capuano, B., and Lane, J. R. (2014) Biased Agonism at G Protein-Coupled Receptors: The Promise and the Challenges-A Medicinal Chemistry Perspective, *Med Res Rev*.
4. Congreve, M., Dias, J. M., and Marshall, F. H. (2014) Structure-based drug design for G protein-coupled receptors, *Prog Med Chem* 53, 1-63.
5. Hollenstein, K., de Graaf, C., Bortolato, A., Wang, M. W., Marshall, F. H., and Stevens, R. C. (2014) Insights into the structure of class B GPCRs, *Trends Pharmacol Sci* 35, 12-22.
6. Christopoulos, A. (2014) Advances in GPCR Allostery: From Function to Structure, *Mol Pharmacol*.
7. Blazer, L. L., and Neubig, R. R. (2009) Small molecule protein-protein interaction inhibitors as CNS therapeutic agents: current progress and future hurdles, *Neuropsychopharmacology* 34, 126-141.
8. Neubig, R. R., and Siderovski, D. P. (2002) Regulators of G-protein signalling as new central nervous system drug targets, *Nat Rev Drug Discov* 1, 187-197.
9. Sjogren, B., Blazer, L. L., and Neubig, R. R. (2010) Regulators of G protein signaling proteins as targets for drug discovery, *Prog Mol Biol Transl Sci* 91, 81-119.
10. Traynor, J. R., and Neubig, R. R. (2005) Regulators of G protein signaling & drugs of abuse, *Mol Interv* 5, 30-41.
11. Bodle, C. R., Mackie, D. I., and Roman, D. L. (2013) RGS17: an emerging therapeutic target for lung and prostate cancers, *Future Med Chem* 5, 995-1007.
12. Kimple, A. J., Bosch, D. E., Giguere, P. M., and Siderovski, D. P. (2011) Regulators of G-protein signaling and their Galpha substrates: promises and challenges in their use as drug discovery targets, *Pharmacol Rev* 63, 728-749.
13. Sjogren, B. (2011) Regulator of G protein signaling proteins as drug targets: current state and future possibilities, *Adv Pharmacol* 62, 315-347.
14. Chen, Y., Liu, Y., Cottingham, C., McMahon, L., Jiao, K., Greengard, P., and Wang, Q. (2012) Neurabin scaffolding of adenosine receptor and RGS4 regulates anti-seizure effect of endogenous adenosine, *J Neurosci* 32, 2683-2695.
15. Lerner, T. N., and Kreitzer, A. C. (2012) RGS4 Is Required for Dopaminergic Control of Striatal LTD and Susceptibility to Parkinsonian Motor Deficits, *Neuron* 73, 347-359.
16. Ko, W. K., Martin-Negrier, M. L., Bezard, E., Crossman, A. R., and Ravenscroft, P. (2014) RGS4 is involved in the generation of abnormal involuntary movements in the unilateral 6-OHDA-lesioned rat model of Parkinson's disease, *Neurobiol Dis* 70, 138-148.
17. Azzarito, V., Long, K., Murphy, N. S., and Wilson, A. J. (2013) Inhibition of alpha-helix-mediated protein-protein interactions using designed molecules, *Nat Chem* 5, 161-173.
18. London, N., Raveh, B., and Schueler-Furman, O. (2013) Druggable protein-protein interactions--from hot spots to hot segments, *Curr Opin Chem Biol* 17, 952-959.

19. Voet, A., Banwell, E. F., Sahu, K. K., Heddle, J. G., and Zhang, K. Y. (2013) Protein interface pharmacophore mapping tools for small molecule protein: protein interaction inhibitor discovery, *Curr Top Med Chem* 13, 989-1001.
20. Morelli, X., Bourgeas, R., and Roche, P. (2011) Chemical and structural lessons from recent successes in protein-protein interaction inhibition (2P2I), *Curr Opin Chem Biol* 15, 475-481.
21. Mullard, A. (2012) Protein-protein interaction inhibitors get into the groove, *Nature Reviews Drug Discovery* 11, 173-175.
22. Villoutreix, B. O., Labbe, C. M., Lagorce, D., Laconde, G., and Sperandio, O. (2012) A leap into the chemical space of protein-protein interaction inhibitors, *Curr Pharm Des* 18, 4648-4667.
23. Kalgutkar, A. S., and Dalvie, D. K. (2012) Drug discovery for a new generation of covalent drugs, *Expert Opin Drug Discov* 7, 561-581.
24. Lopez-Tarruella, S., Jerez, Y., Marquez-Rodas, I., and Martin, M. (2012) Neratinib (HKI-272) in the treatment of breast cancer, *Future Oncol* 8, 671-681.
25. Blazer, L. L., Zhang, H., Casey, E. M., Husbands, S. M., and Neubig, R. R. (2011) A nanomolar-potency small molecule inhibitor of Regulator of G protein Signaling (RGS) proteins, *Biochemistry*.
26. Turner, E. M., Blazer, L. L., Neubig, R. R., and Husbands, S. M. (2012) Small Molecule Inhibitors of Regulator of G Protein Signalling (RGS) Proteins, *ACS Med Chem Lett* 3, 146-150.
27. Rosa, A. O., Kaster, M. P., Binfare, R. W., Morales, S., Martin-Aparicio, E., Navarro-Rico, M. L., Martinez, A., Medina, M., Garcia, A. G., Lopez, M. G., and Rodrigues, A. L. (2008) Antidepressant-like effect of the novel thiadiazolidinone NP031115 in mice, *Prog Neuropsychopharmacol Biol Psychiatry* 32, 1549-1556.
28. Castro, A., Encinas, A., Gil, C., Brase, S., Porcal, W., Perez, C., Moreno, F. J., and Martinez, A. (2008) Non-ATP competitive glycogen synthase kinase 3beta (GSK-3beta) inhibitors: study of structural requirements for thiadiazolidinone derivatives, *Bioorg Med Chem* 16, 495-510.
29. Martinez, A., Alonso, M., Castro, A., Perez, C., and Moreno, F. J. (2002) First non-ATP competitive glycogen synthase kinase 3 beta (GSK-3beta) inhibitors: thiadiazolidinones (TDZD) as potential drugs for the treatment of Alzheimer's disease, *J Med Chem* 45, 1292-1299.
30. Wang, Q., Liu-Chen, L. Y., and Traynor, J. R. (2009) Differential modulation of mu- and delta-opioid receptor agonists by endogenous RGS4 protein in SH-SY5Y cells, *J Biol Chem* 284, 18357-18367.
31. Besnard, J., Ruda, G. F., Setola, V., Abecassis, K., Rodriguiz, R. M., Huang, X. P., Norval, S., Sassano, M. F., Shin, A. I., Webster, L. A., Simeons, F. R., Stojanovski, L., Prat, A., Seidah, N. G., Constam, D. B., Bickerton, G. R., Read, K. D., Wetsel, W. C., Gilbert, I. H., Roth, B. L., and Hopkins, A. L. (2012) Automated design of ligands to polypharmacological profiles, *Nature* 492, 215-220.
32. Fenalti, G., Giguere, P. M., Katritch, V., Huang, X. P., Thompson, A. A., Cherezov, V., Roth, B. L., and Stevens, R. C. (2014) Molecular control of delta-opioid receptor signalling, *Nature* 506, 191-196.
33. Wu, H., Wacker, D., Mileni, M., Katritch, V., Han, G. W., Vardy, E., Liu, W., Thompson, A. A., Huang, X. P., Carroll, F. I., Mascarella, S. W., Westkaemper, R. B., Mosier, P. D., Roth, B. L., Cherezov, V., and Stevens, R. C. (2012) Structure of the human kappa-opioid receptor in complex with JDTic, *Nature* 485, 327-332.
34. Cifelli, C., Rose, R. A., Zhang, H., Voigtlaender-Bolz, J., Bolz, S. S., Backx, P. H., and Heximer, S. P. (2008) RGS4 regulates parasympathetic signaling and heart rate control in the sinoatrial node, *Circ Res* 103, 527-535.

- 1
2
3 35. Vashisth, H., Storaska, A. J., Neubig, R. R., and Brooks, C. L., 3rd. (2013) Conformational
4 dynamics of a regulator of G-protein signaling protein reveals a mechanism of allosteric
5 inhibition by a small molecule, *ACS Chem Biol* 8, 2778-2784.
- 6
7 36. Fu, Y., Huang, X., Zhong, H., Mortensen, R. M., D'Alecy, L. G., and Neubig, R. R. (2006)
8 Endogenous RGS proteins and Galpha subtypes differentially control muscarinic and adenosine-
9 mediated chronotropic effects, *Circ Res* 98, 659-666.
- 10
11 37. Roman, D. L., Ota, S., and Neubig, R. R. (2009) Polyplexed Flow Cytometry Protein Interaction
12 Assay: A Novel High-Throughput Screening Paradigm for RGS Protein Inhibitors, *J Biomol*
13 *Screen* 14, 610-619.
- 14
15 38. Storaska, A. J., Mei, J. P., Wu, M., Li, M., Wade, S. M., Blazer, L. L., Sjogren, B., Hopkins, C.
16 R., Lindsley, C. W., Lin, Z., Babcock, J. J., McManus, O. B., and Neubig, R. R. (2013)
17 Reversible inhibitors of regulators of G-protein signaling identified in a high-throughput cell-
18 based calcium signaling assay, *Cell Signal* 25, 2848-2855.
- 19
20 39. Blazer, L. L., Roman, D. L., Muxlow, M. R., and Neubig, R. R. (2010) Use of flow cytometric
21 methods to quantify protein-protein interactions, *Curr Protoc Cytom Chapter 13*, Unit 13 11 11-
22 15.
- 23
24 40. Roman, D. L., Talbot, J. N., Roof, R. A., Sunahara, R. K., Traynor, J. R., and Neubig, R. R.
25 (2007) Identification of small-molecule inhibitors of RGS4 using a high-throughput flow
26 cytometry protein interaction assay, *Mol Pharmacol* 71, 169-175.
- 27
28 41. Zielinski, T., Kimple, A. J., Hutsell, S. Q., Koeff, M. D., Siderovski, D. P., and Lowery, R. G.
29 (2009) Two Galpha(i1) rate-modifying mutations act in concert to allow receptor-independent,
30 steady-state measurements of RGS protein activity, *J Biomol Screen* 14, 1195-1206.
- 31
32 42. Chang, L., Bertelsen, E. B., Wisen, S., Larsen, E. M., Zuiderweg, E. R., and Gestwicki, J. E.
33 (2008) High-throughput screen for small molecules that modulate the ATPase activity of the
34 molecular chaperone DnaK, *Anal Biochem* 372, 167-176.
- 35
36 43. Marti, M., Trapella, C., Viaro, R., and Morari, M. (2007) The nociceptin/orphanin FQ receptor
37 antagonist J-113397 and L-DOPA additively attenuate experimental parkinsonism through
38 overinhibition of the nigrothalamic pathway, *J Neurosci* 27, 1297-1307.
- 39
40 44. Viaro, R., Sanchez-Pernaute, R., Marti, M., Trapella, C., Isacson, O., and Morari, M. (2008)
41 Nociceptin/orphanin FQ receptor blockade attenuates MPTP-induced parkinsonism, *Neurobiol*
42 *Dis* 30, 430-438.
- 43
44 45. Sanberg, P. R., Bunsey, M. D., Giordano, M., and Norman, A. B. (1988) The catalepsy test: its
45 ups and downs, *Behav Neurosci* 102, 748-759.
- 46
47 46. Schallert, T., De Ryck, M., Wishaw, I. Q., Ramirez, V. D., and Teitelbaum, P. (1979) Excessive
48 bracing reactions and their control by atropine and L-DOPA in an animal analog of
49 Parkinsonism, *Exp Neurol* 64, 33-43.
- 50
51
52
53
54
55
56
57
58
59
60



20
21
22
23
24
25
26
27
28
29
30
31
32
33
34
35
36
37
38
39
40
41
42
43
44
45
46
47
48
49
50
51
52
53
54
55
56
57
58
59
60

TOC Graphic

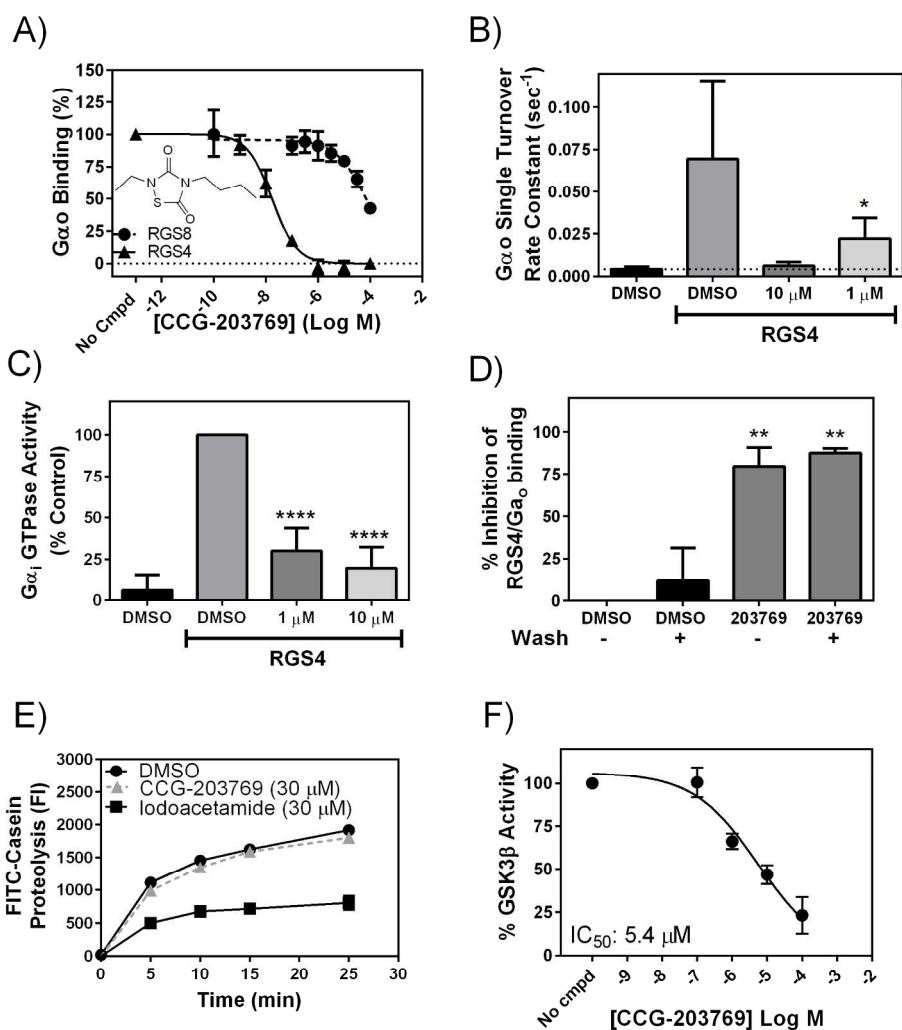


Figure 1: Biochemical characterization of RGS inhibitors. A) CCG-203769 inhibits RGS4 and RGS8 binding to Gαo in FCPIA in a concentration-dependent manner. Inset: chemical structure of CCG-203769. See Table 1 for IC₅₀ values. CCG-203769 inhibits the RGS-mediated acceleration of GTPase activity by both B) Gαo in single-turnover and C) Gαi1 in steady-state GTPase assays. D) CCG-203769 irreversibly inhibits RGS4 binding to Gαo in non-reducing buffers. RGS4-coated beads were treated with 0.5 μM CCG-203769, extensively washed, and then probed for Gαo binding. E) CCG-203769 (30 μM) does not inhibit the cysteine protease papain. The positive control compound, iodoacetamide (30 μM) did effectively inhibit papain activity (see Methods for details). F) CCG-203769 inhibits GSK-3β with an IC₅₀ value of 5 μM. Data are presented as the mean±SEM from at least three independent experiments. * p<0.05, ****p<0.0001

201x217mm (300 x 300 DPI)

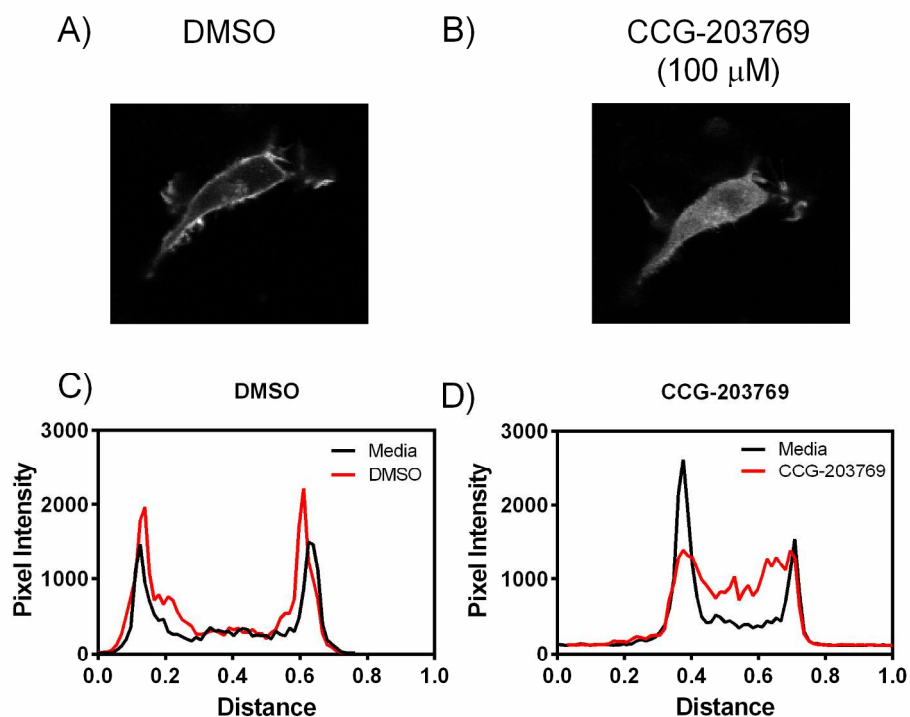


Figure 2: CCG-203769 inhibits the Gao-dependent membrane translocation of RGS4 in HEK293T cells. RGS4-GFP generally has a diffuse cytosolic protein expression pattern, however, co-expression with Gao induces a translocation of the RGS to the cell membrane(25). A/C) Treatment with DMSO does not modulate the RGS4 membrane localization, while B/D) treatment with CCG-203769 (100 μ M) reverses the membrane translocation of the RGS4. Representative data shown from at least three independent experiments with 3-5 cells imaged per experiment. Line scans (C & D) were quantified from a single line perpendicular to the long axis of the cell in pre (Media) & post (DMSO or CCG-203769) treatment images. Pixel intensity was obtained using the NIH ImageJ software version 1.43r.
203x155mm (300 x 300 DPI)

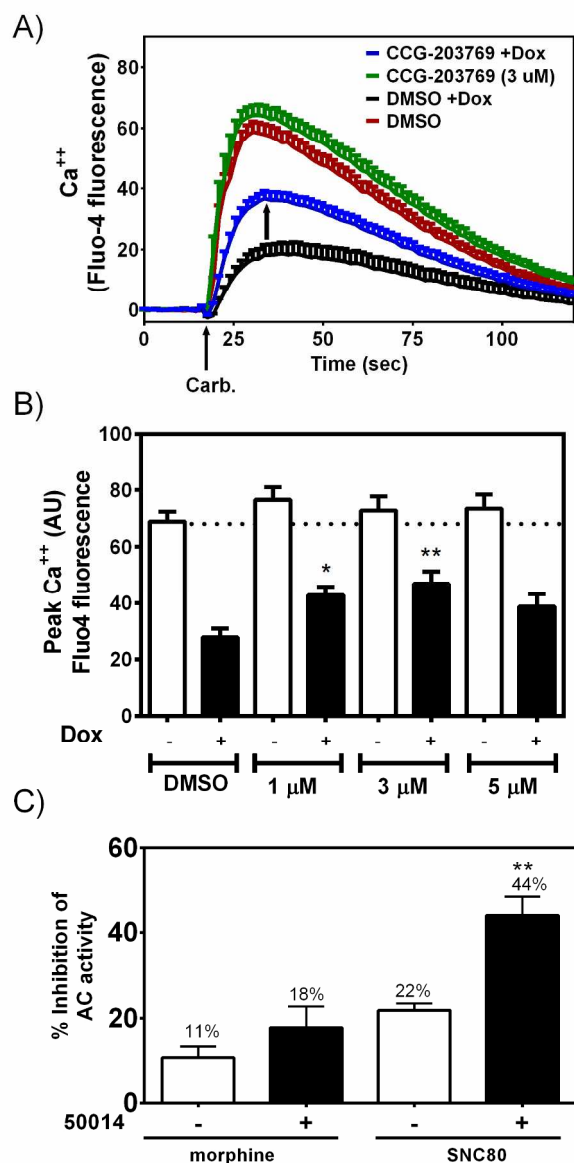


Figure 3. TDZD RGS4 inhibitors block RGS function in living cells. A) RGS4 induction by doxycycline suppresses the $\text{G}\alpha_q$ -mediated calcium transient invoked by activation of the M3 muscarinic receptor. CCG-203769 (3 μM) reverses the effect of RGS4. B) Quantification of the data shown in A, showing that CCG-203769 significantly inhibits the RGS4 modulation M3 signaling at 1 and 3 μM . Data are presented as the mean \pm SEM of three independent experiments. C) δ -opioid receptor signaling in SH-SY5Y neuroblastoma cells is potentiated by the TDZD RGS4 inhibitor. The endogenous δ and μ receptors in SH-SY5Y cells are regulated by endogenous RGS proteins. CCG-50014 (100 μM) significantly potentiates the cAMP inhibition produced by the δ opioid receptor agonist SNC-80, while only modestly potentiating actions of the μ -opioid receptor agonist morphine. Data are presented as the mean \pm SEM of three independent experiments. * $p < 0.05$; ** $p < 0.01$
158x267mm (300 x 300 DPI)

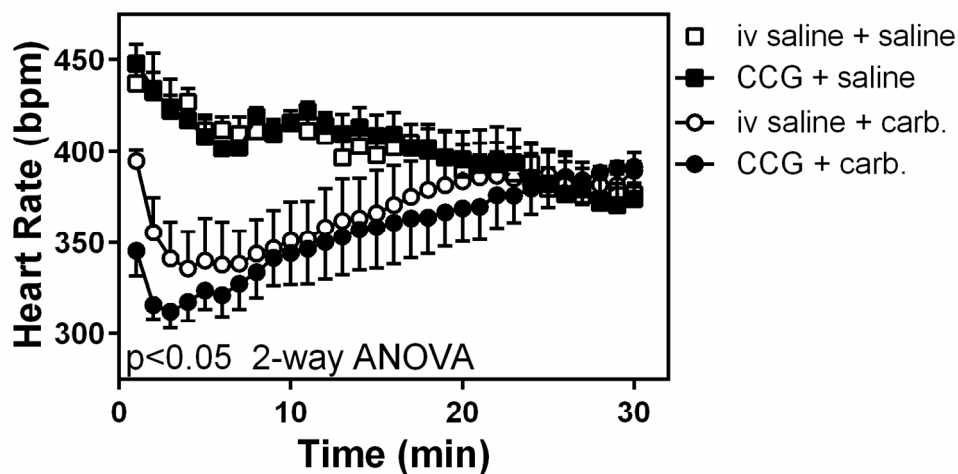


Figure 4. CCG-203769 potentiates the cardiovascular effects of carbachol in conscious rats. Blood pressure and heart rate of adult Sprague-Dawley rats were monitored via indwelling cardiac transponders. Rats were given CCG-203769 (10mg/kg, i.v.) or saline immediately before administration of saline or carbachol (0.1mg/kg, i.p.). CCG-203769 has no effect on heart rate when administered alone, however it significantly potentiates ($p < 0.05$, 2-way ANOVA) the effect of carbachol (0.1mg/kg). N=6 per condition.
138x75mm (300 x 300 DPI)

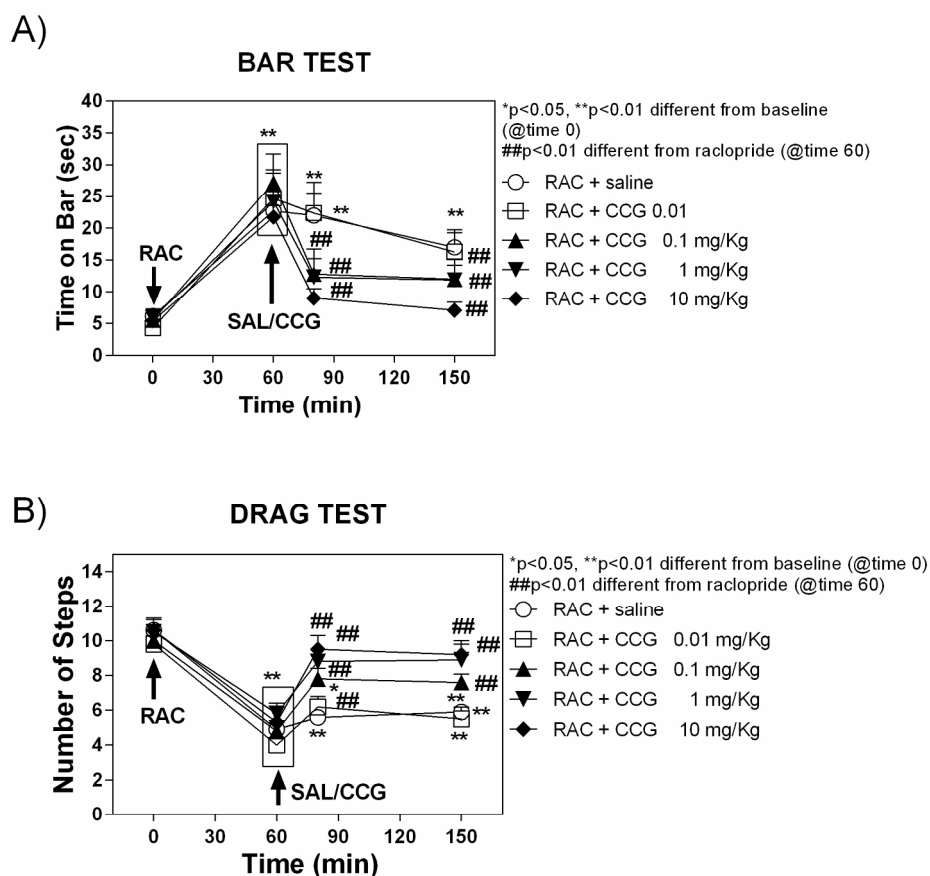


Figure 5. AntiParkinson's effects of RGS4 inhibitors. Mice were treated with raclopride (1 mg/kg i.p.) after baseline assessment in the bar and drag tests (as described in Materials and Methods). A) Akinesia and B) bradykinesia were assessed 30 minutes after raclopride then mice received either DMSO or CCG-203769 at the indicated doses (i.p.). Behavior was assessed 20 or 90 minutes after DMSO or CCG-203769. Values are mean +/- SEM with differences from baseline indicated by ** ($p < 0.01$) and differences from Raclopride + DMSO indicated by ## ($p < 0.01$).

194x179mm (300 x 300 DPI)